The Jacobi diffusion process as a neuronal model

(Article begins on next page)

19 April 2024

AIP/123-QED

The Jacobi diffusion process as a neuronal model

G. D'Onofrio,[1, a)] M.Tamborrino,[2, b)] and P. Lansky[1, c)]

[1)]*Institute of Physiology of the Czech Academy of Sciences, Videnska 1083,*

14220 Prague 4, Czech Republic

[2)]*Johannes Kepler University Linz, Altenbergerstraße 69, 4040 Linz,*

Austria

The Jacobi process is a stochastic diffusion characterized by a linear drift and a special form of multiplicative noise which keeps the process confined between two boundaries. One example of such a process can be obtained as the diffusion limit of the Stein's model of membrane depolarization which includes both, excitatory and inhibitory reversal potentials. The reversal potentials create the two boundaries between which the process is confined. Solving the first-passage-time problem for the Jacobi process, we found closed-form expressions for mean, variance and third moment, that are easy to implement numerically. The first two moments are used here to determine the role played by the parameters of the neuronal model. Namely, the effect of multiplicative noise on the output of the Jacobi neuronal model with input-dependent parameters is examined in detail and compared with the properties of the generic Jabobi diffusion. It appears that the dependence of the model parameters on the rate of inhibition turns out to be of primary importance to observe a change in the slope of the response curves. This dependence also affects the variability of the output as reflected by the coefficient of variation. It often takes values larger than one and it is not always a monotonic function in dependency on the rate of excitation.

[a)]Electronic mail: giuseppe.donofrio@unito.it

[b)]Electronic mail: massimiliano.tamborrino@jku.at

[c)]Electronic mail: lansky@biomed.cas.cz

Diffusion processes with multiplicative noise are able to model the changes in the membrane depolarization between two consecutive spikes of a single neuron. Among them, the most commonly used models consider either no state-space boundaries or only a lower boundary. Nevertheless, the upper boundary also modifies the properties of the model due to the multiplicativity of the noise. Here we consider the Jacobi diffusion process that is able to include, in its neuronal interpretation, both excitatory and inhibitory reversal potentials (upper and lower boundary, respectively). In the Jacobi neuronal model the involved parameters are input-dependent and this, together with the form of the multiplicative noise, affects the output of the model. The response of the neuron is studied focusing on the behavior of the first-passage time through the firing threshold, identified with the dynamics of spike generation. Computationally easy expressions of the first two moments of the first-passage time for the Jacobi process are derived and implemented to study the firing rate and variability of the inter-spike intervals. The third moment is given as a tool for the parameter estimation. All the results concerning the first-passage-time problem are general and can be used outside the framework of computational neuroscience.

I.   INTRODUCTION

In the models where noise is assigned a casual importance, it is often assumed to be a source of inefficiency and unpredictability. However, there exists a large class of phenomena for which the noise is of a primary importance or even a part of the signal itself. Mathematical models in neuroscience are one of the most prominent examples in this direction. The celebrated model of Lapicque, republished and discussed at its centennial anniversary[1,2], was deterministic, but its numerous generalizations took into account the input-output variability of the neurons in the networks and became intrinsically stochastic. From a biophysical point of view, the models of a single neuron reflect the electrical properties of its membrane. Such circuit models can be written in terms of differential equations for the membrane voltage. To reduce their mathematical complexity, integrate-and-fire type of the models have been derived[3,4]. These models aim to describe the dynamics of interspike intervals and

they are based on a one-dimensional representation of the time evolution of the neuronal membrane depolarization.

One class of stochastic models which can be classified as a generalization of the Lapicque model with restricted state space appeared in the sixties. Stein[5] and Johannesma[6] introduced models with conductance changes caused by excitatory and inhibitory inputs. The state space of the depolarization was limited between two boundaries, the inhibitory and the excitatory reversal potentials. Later, this type of models with multiplicative noise started to be extensively investigated[7–11]. These studies often employed the diffusion limits of the originally discontinuous models to improve their tractability. Among them, the most commonly investigated model considers the lower boundary only and with its specific form of the diffusion coefficient, it can be identified as the Feller process (in biology), also known as Cox-Ingersoll-Ross (in finance) or square-root process (in mathematics). Nevertheless, there seems to be no strong mathematical argument for the selection of a specific form of the diffusion coefficient which controls the state space of the depolarization. Thus, several other different variants have been investigated[11,12]. The emphasis on the lower boundary, the inhibitory reversal potential, appears probably because the role of the upper boundary, the excitatory reversal potential, seems to be blurred by imposing below it a firing threshold. However, despite the existence of the threshold, the upper boundary modifies the properties of the model due to the multiplicativity of the noise.

The studies in which both reversal potentials are considered are more rare[13–16] and the present article is devoted to such a model. Here, the effect of multiplicative noise on the output of Jacobi neuronal model with dependent parameters is examined in detail. After introducing the Jacobi diffusion process and describing the firing mechanism which is based on the solution of the first-passage-time problem, the expressions for the first three moments are presented. Up to this point, the results are independent of the application in neuroscience. Further, intrinsic dependency of the parameters as it follows from biophysical model is presented and results for such a model deduced and interpreted.

II.   THE PEARSON DIFFUSION MODELS

One-dimensional stochastic differential equations play a key role in the description of fluctuating phenomena belonging to different fields of applications as physics, biology, neu-

science, finance and others[17]. In particular, the class of models with a linear drift and driven by a Wiener process is widely used for its mathematical tractability and flexibility. These models are described by a stochastic differential equation of the following type

$$dY_t = (-\alpha Y_t + \beta)\, dt + \Sigma(Y_t)dW_t, \quad Y_0 = y_0, \tag{1}$$

where $\alpha > 0$, $\beta \in \mathbb{R}$, $W = \{W_t\}_{t \geq 0}$ is a standard Wiener process and $Y_0 = y_0$ is the initial condition. The diffusion coefficient $\Sigma(Y_t) > 0$ determines the amplitude of the noise and, according to its dependence on Y_t, it characterizes the solution of Eq.(1). If $\Sigma(Y_t) = \sqrt{aY_t^2 + bY_t + c}$ for $a, b, c \in \mathbb{R}$, the solution of Eq.(1) is called Pearson diffusion process[18]. A wide range of well-known processes belongs to this class. The solution of Eq.(1) is an Ornstein-Uhlenbeck process for $\Sigma(Y_t) = \sigma > 0$ constant (i.e. $a = b = 0, c = \sigma$), a Feller process (also known as Cox-Ingersoll-Ross model or square-root process) for $\Sigma(Y_t) = \sigma_F \sqrt{Y_t}, \sigma_F > 0$ (i.e. $b = \sigma_F^2, a = c = 0$), an inhomogeneous geometric Brownian motion for $\Sigma(Y_t) = \sigma_G Y_t, \sigma_G > 0$ (i.e. $a = \sigma_G^2, b = c = 0$) and a Jacobi diffusion (or Wright-Fisher diffusion process) for $\Sigma(Y_t) = \sigma_J \sqrt{Y_t(1 - Y_t)}$ (i.e. $a = -\sigma_J^2, b = \sigma_J^2, c = 0$). Throughout this work we will focus on this last process.

The values taken by model (1), i.e. its state space, are in the interval $-\infty \leq B_1 < y_0 < B_2 \leq +\infty$. The endpoints B_1 and B_2 can or cannot be reached in a finite time depending on the underlying parameter conditions. According to the Feller's classification of boundaries[19], B_1 is an entrance boundary if it cannot be reached by Y_t in finite time, and there is no probability flow to the outside of the interval $(B_1, +\infty)$, that is, the process stays in $[B_1, +\infty)$ with probability 1. Vice versa, B_1 is an exit boundary if the process can attain it, but then it cannot return into $(B_1, +\infty)$. The latter situation is not suitable for our modeling purposes, and thus it is not considered here. An analogous classification for B_2 can be stated.

We denote the transition probability density function (pdf) of the diffusion process (1) by $f(y, t|z, \tau)$. If $\mathcal{W}(y) := \lim_{t \to \infty} f(y, t|y_0, 0)$ exists independently on y_0, we say that the process Y_t admits a stationary distribution $\mathcal{W}(y)$. Independently on the choice of $\Sigma(Y_t)$, the mean of Y_t in (1) is given by

$$\mathbb{E}[Y_t|Y_0 = y_0] = \frac{\beta}{\alpha} + \left(y_0 - \frac{\beta}{\alpha}\right)e^{-\alpha t}, \tag{2}$$

4

and the asymptotic mean by

$$\lim_{t \to +\infty} \mathbb{E}[Y_t | Y_0 = y_0] := \mathbb{E}[Y_\infty] = \frac{\beta}{\alpha}, \tag{3}$$

while higher moments of Y_t depend on the function $\Sigma(Y_t)$ in (1).

Let the process Y_t evolve in the presence of an absorbing boundary S, $y_0 < S < B_2$. Then Eq.(1) describes the dynamics of Y_t until it crosses S for the first time, the so called first-passage time (FPT), defined as

$$T := \inf\{t \geq 0 : Y_t \geq S | y_0 < S\}, \tag{4}$$

with pdf $g(t) := g(t | y_0, S)$. The moments of T can be calculated through the Siegert's formula[20]

$$\mathbb{E}[T^n] = n \int_{x_0}^{S} \frac{2dz}{[\Sigma(Y_t)]^2 \mathcal{W}(z)} \int_{-\infty}^{z} \mathcal{W}(x) \mathbb{E}[T^{n-1}] dx, \quad n = 1, 2, \dots \tag{5}$$

Three distinct situations for the FPT can occur. The process is said to be in the suprathreshold, subthreshold and threshold regimes if $\mathbb{E}[Y_\infty] > S, \mathbb{E}[Y_\infty] < S$ and $\mathbb{E}[Y_\infty] = S$, respectively.

A. The Jacobi diffusion process

The aforementioned Jacobi diffusion[19] is a stochastic process with state space $(0, 1)$, given as the solution to the following stochastic differential equation

$$dY_t = (-\alpha Y_t + \beta)dt + \sigma \sqrt{Y_t(1 - Y_t)} dW_t, \quad Y_0 = y_0, \tag{6}$$

with $\alpha > 0, \sigma > 0, y_0 \in (0, 1)$. Sometimes, it is alternatively defined on the interval $(-1, 1)$ by setting $\Sigma(Y_t) = \sigma_J \sqrt{1 - Y_t^2}, \sigma_J > 0$. Throughout, we will consider the Jacobi diffusion given by (6). The conditional variance of the Jacobi process, the moment generating function and the transition pdf are given in Refs.18, 21 and 22, respectively.

Let $\eta := 2\alpha/\sigma^2$ and $\gamma := 2\beta/\sigma^2$. Then, for $\gamma > 0$ such that $\min(\gamma, \eta - \gamma) \geq 1$, the boundaries 0 and 1 are of entrance type[22] and the Jacobi diffusion admits a stationary distribution $\mathcal{W}$. In particular, $\mathcal{W}$ is a Beta-distribution with shape parameter γ and scale parameter $\eta - \gamma$, i.e.[18]

$$Y_\infty \sim \text{Beta}(\gamma, \eta - \gamma), \tag{7}$$

5

with mean (3) and variance $\text{Var}(Y_\infty) = \beta(\alpha - \beta)\sigma^2/(2\alpha + \sigma^2)$.

In the presence of a constant threshold S, with $0 < y_0 < S < 1$, the Laplace transform of the FPT T, i.e. $g^*(\xi) := \mathbb{E}[e^{-\xi T}] = \int_0^\infty e^{-\xi t} g(t) dt, \xi > 0$, is given by[21]

$$g^*(\xi) = \frac{{}_2F_1\left(\frac{2\xi}{\theta\sigma^2}, \theta; \gamma; y_0\right)}{{}_2F_1\left(\frac{2\xi}{\theta\sigma^2}, \theta, \gamma; S\right)}, \tag{8}$$

where

$$\theta = \frac{2\alpha - \sigma^2 - \sqrt{(\sigma^2 - 2\alpha)^2 - 8\xi\sigma^2}}{2\sigma^2}.$$

Here ${}_2F_1$ denotes the Gaussian hypergeometric function belonging to the class of the generalized hypergeometric functions ${}_pF_q$ defined by

$${}_pF_q(a_1, \ldots, a_p; b_1, \ldots, b_q; z) := \sum_{n=0}^\infty \frac{(a_1)_n \cdots (a_p)_n}{(b_1)_n \cdots (b_q)_n} \frac{z^n}{n!}, \tag{9}$$

where $(a)_n$ is the rising factorial defined by $(a)_n = a(a+1)\cdots(a+n-1)$ for $n \in \mathbb{N}$ and $(a)_0 = 1$. The mean FPT, $\mathbb{E}[T]$, is[21]

$$\mathbb{E}[T] = \frac{1}{\beta} \sum_{k=0}^\infty \frac{(\eta)_k}{(\gamma+1)_k} \frac{S^{k+1} - y_0^{k+1}}{k+1}. \tag{10}$$

Using the definition of the hypergeometric function (9) for $p = 3$ and $q = 2$, and the fact that $(1)_k = k!, (2)_k = (k+1)!$, we rewrite Eq.(10) as

$$\mathbb{E}[T] = \frac{1}{\beta} \left[{}_3F_2\left(1, 1, \eta; 2, \gamma+1; S\right) S - {}_3F_2\left(1, 1, \eta; 2, \gamma+1; y_0\right) y_0\right]. \tag{11}$$

This expression involves only hypergeometric functions, and has the advantage of easier numerical evaluations with the package *hypergeo*[23] in the computing environment $\mathbf{R}$[24].

We derive the second moment of T using the Siegert formula (5) and replacing the integral terms with their Taylor expansions, following what has been proposed in Ref. 25 for the calculation of the moments of the FPT of an Ornstein-Uhlenbeck process. In this way we obtain the variance of T

$$\text{Var}(T) = \frac{\mathbb{E}[T]}{\beta} \left[S \, {}_3F_2\left(1, 1, \eta; 2, \gamma+1; S\right) + y_0 \, {}_3F_2\left(1, 1, \eta; 2, \gamma+1; y_0\right)\right] + \tag{12}$$

$$-\frac{4}{\sigma^2\beta} \sum_{k=0}^\infty \frac{(\eta)_k}{(\gamma+1)_k(k+1)(k+2)(\gamma+k+1)} \times$$

$$\times \left[{}_3F_2(1, k+2, \eta+k+1; k+3, \gamma+k+2; S)S^{k+2} - {}_3F_2(1, k+2, \eta+k+1; k+3, \gamma+k+2; y_0)y_0^{k+2}\right].$$

To evaluate Eq.(12) numerically, we replace the series with the sum of the first k terms. Our comparisons for different values of k with Monte Carlo simulations show that the series

(and thus the value of the variance) can be satisfactorily computed by summing the first 20 terms. All the numerical results presented in the following parts were carefully verified by extensive simulations with relative difference always below 1%. Finally, we also derive the third moment of T using the Siegert formula (5), obtaining

$$
\begin{aligned}
\mathbb{E}[T^3] = &\frac{3S\mathbb{E}[T^2]}{\beta} \; {}_3F_2\left(1, 1, \eta; 2, \gamma + 1; S\right) + \\
&- 12\frac{\mathbb{E}[T]}{\sigma^2\beta} \sum_{k=0}^{\infty} \frac{(\eta)_k \; {}_3F_2(1, k+2, \eta+k+1; k+3, \gamma+k+2; S)S^{k+2}}{(\gamma+1)_k(k+1)(k+2)(\gamma+k+1)} + \\
&+ \frac{24}{\sigma^4\beta} \sum_{k=0}^{\infty} \frac{(\eta)_k}{(\gamma+1)_k(k+1)(\gamma+k+1)} \sum_{n=0}^{\infty} \frac{(\eta+k+1)_n}{(\gamma+k+2)_n(k+n+2)(\gamma+k+n+2)} \times \\
&\times \Big[{}_3F_2\left(1, k+n+3, \eta+k+n+2; k+n+4, \gamma+k+n+3; S\right)S^{k+n+3} + \\
&\quad - {}_3F_2\left(1, k+n+3, \eta+k+n+2; k+n+4, \gamma+k+n+3; y_0\right)y_0^{k+n+3}\Big].
\end{aligned}
$$

The derived expressions of the first three moments can be used to perform moment estimation of the parameters α, β and σ appearing in Eq.(6). This would be particularly interesting in neuroscience, where parameter estimation from FPT data has already been successfully applied for other diffusion models[26–29]. Moreover, it will allow a comparison with the results available for the parameter inference on α and β for the Jacobi process for continuously recorded observations of the trajectory of $X(t)$ (modeling the membrane voltage)[30].

In Fig. 1, we illustrate the inverse mean FPT, defined as $1/\mathbb{E}[T]$, the coefficient of variation (CV) of T, defined as the ratio between the standard deviation and the mean of T, i.e. $\text{CV}(T) = \sqrt{\text{Var}(T)}/\mathbb{E}[T]$, and the stationary distribution $\mathcal{W}$ of the Jacobi diffusion (6) given by Eq.(7). As expected, the inverse mean FPT increases and CV decreases with increasing drift coefficient, β. Further, the asymptotic distribution gets more symmetric for large values of β. Both, the inverse mean FPT as well as CV, increase with increasing the noise amplitude and the curves become smoother.

B. The Jacobi diffusion as a neuronal model

Eq.(1) with various noisy terms is widely used in the context of neuroscience. It describes the subthreshold dynamics of the membrane voltage of a nerve cell, i.e. the evolution of the membrane depolarization between two consecutive spikes (firing), modeled as crossings of a certain threshold. In this way the interspike interval (ISI) is identified with the FPT of
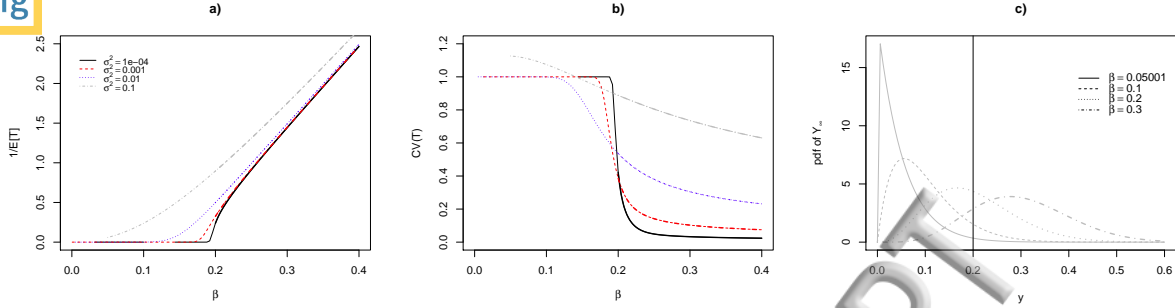
FIG. 1. Some properties of the Jacobi diffusion. Panels (a) and (b): Inverse mean FPT and $CV(T)$ as a function of the drift coefficient, β, for different values of the noise, σ^2. The process is in suprathreshold regime for $\beta > 0.2$ (thick lines). In both figures, $y_0 = 0.1$, $\alpha = 1$, $S = 0.2$. Panel (c): pdf of the asymptotic distribution $\mathcal{W}$ of Y_∞ for different values of β with $y_0 = 0.1$, $\alpha = 1$ and $\sigma^2 = 0.1$. Values of $\beta \leq 0.05$ do not satisfy the condition $\min(\gamma, \eta - \gamma) \geq 1$ in this case. The vertical line represents the threshold S.

the mathematical model. With $\Sigma(Y_t) = 0$, constant absorbing threshold S, time constant $\tau = 1/\alpha$ and constant or time-varying input β, Eq.(1) has often been investigated as a deterministic leaky integrate-and-fire neuronal model[31]. To take the underlying intrinsic neuronal randomness into account, the model was often extended by adding a white or colored noise.

The diffusion process (1) has been often obtained as a diffusion limit (also known as diffusion approximation) of discontinuous jump process under the assumption of increasing frequency and decreasing size of the jumps[9,11,32,33]. An example of the initial discontinuous process is the Stein's model with reversal potentials V_I and V_E given by the following stochastic differential equation:

$$dX_t = -\frac{1}{\tau}X_t dt + a(V_E - X_t)dN^+(t) + i(X_t - V_I)dN^-(t), \qquad X_0 = x_0, \qquad (13)$$

where i and a are constants such that $-1 < i < 0 < a < 1$. Here $\tau > 0$ is the membrane constant taking into account the spontaneous voltage decay towards the resting potential V_R in the absence of input and the inhibitory and excitatory reversal potentials V_I and V_E are such that $V_I < 0 < V_E$. We assume $V_R = x_0 = 0$. In Eq.(13), $N^+ := \{N^+(t), t \geq 0\}$ and $N^- := \{N^-(t), t \geq 0\}$ are two independent homogeneous Poisson processes with $N^+(0) = N^-(0) = 0$ and intensities λ and ω, respectively. The processes N^+ and N^-

8

represent the excitatory and inhibitory neuronal inputs, respectively, while λ and ω are called the excitatory and inhibitory input parameters and represent the rate of arrival of excitatory and inhibitory postsynaptic potentials. According to model (13), each event of the excitatory process N^+ produces a jump in the membrane voltage $\Delta X = a(V_E - X_t)$. Similarly, an event of the inhibitory process N^- hyperpolarizes the membrane by $i(X_t - V_I)$. This implies that the effect of the input is state-dependent: the amplitude of changes in the depolarization X_t decreases when X_t approaches the inhibitory or the excitatory reversal potentials V_I and V_E. A direct consequence is that the process is constrained on the interval (V_I, V_E), i.e. the state space of the process is (V_I, V_E).

Under the assumptions of jump amplitudes a, i decreasing to zero but occurring at increasing frequencies λ, ω roughly inversely proportional to the square of the jump size, a diffusion approximation of a generalization of Eq. (13), including random jump amplitudes depending simultaneously on both reversal potentials, was proposed[11]. The stochastic differential equation describing this dynamics is

$$dX_t = \left(-\frac{X_t}{\tau} + \mu(V_E - X_t) + \nu(X_t - V_I)\right) dt + \sigma\sqrt{(V_E - X_t)(X_t - V_I)} dW_t, \quad X_0 = 0, \tag{14}$$

where

$$\mu = a\lambda, \qquad \nu = i\omega. \tag{15}$$

The parameter σ^2 determines the amplitude of the noise and it is often assumed to grow linearly with the input[34–36]. Following this, we let the noise intensity vary according to the formula

$$\sigma^2 = (\lambda + \omega)\epsilon, \tag{16}$$

obtained through the diffusion approximation. Here the constant $\epsilon > 0$ determines the relation between the input parameters and the noise amplitude. The asymptotic depolarization of the process X_t is denoted by X_∞, and its mean is given by

$$\mathbb{E}[X_\infty] = \frac{\mu V_E - \nu V_I}{\frac{1}{\tau} + \nu - \mu}. \tag{17}$$

For a better understanding of the parameters μ and ν, we recall the equation of a conductance-based neuronal model. The evolution in time of the potential difference V across the membrane of a neuron is given by (see e.g. Ref.14 and Ref.37)

$$dV_t = -\frac{g_L}{C} V_t dt - \left[\frac{g_E(t)}{C}(V_t - V_E) + \frac{g_I(t)}{C}(V_t - V_I)\right] dt, \tag{18}$$

9

where C is the membrane capacitance, g_L is the conductance of the leak current, while $g_E(t)$ and $g_I(t)$ are the conductances of the excitatory and inhibitory components of the synaptic current, respectively. Eq.(18) is analogous to Eq.(13) with g_L/C playing the role of the membrane constant τ and with $g_E(t) = Ca_E \sum_k \delta(t - t_k)$, where a_E is a dimensionless constant measuring the strength of the synapse and t_k is the time of the arrival of the k-th incoming excitatory pulse, distributed according to a Poisson process with parameter λ (similarly for $g_I(t)$ and ω). The arrival of one excitatory pulse increases the conductance $g_E(t)$ by a factor of Ca_E and consequently the increase in the voltage is $\Delta V = a_E(V_E - V_t)$.

Focusing again on the model (14), we see that the state space of X_t is again the interval (V_I, V_E), where V_I and V_E are both entrance boundaries if the following condition is satisfied

$$\epsilon(\lambda + \omega) < -\frac{2V_I}{\tau(V_E - V_I)}. \tag{19}$$

Throughout the paper, the underlying parameters are chosen to guarantee that this boundary condition is met.

As previously mentioned, three firing regimes can be considered for the process Y_t and thus for the process X_t. Referring to the latter model, if the asymptotic mean depolarization (17) is larger than the firing threshold S, then the process is in the suprathreshold regime. If it is smaller, then it is in the subthreshold regime and the noise plays a crucial role for the crossing of the threshold. Finally, if the asymptotic mean is equal to S, the process is in the threshold regime. However, due do the interplay of the parameters, the specific situation is more complicated and the role played by the noise may be counterintuitive, as seen later. Using the transformation

$$y = \frac{x - V_I}{V_E - V_I},$$

from Eq.(14) we get Eq.(6), whose solution is confined in $(0, 1)$, with

$$\alpha = \frac{1}{\tau} + \mu - \nu, \qquad \beta = \mu - \frac{V_I}{\tau(V_E - V_I)}, \qquad Y_0 = y_0 = -\frac{V_I}{V_E - V_I}. \tag{20}$$

All the analytical results previously presented for the Jacobi process in $(0, 1)$ can thus be used. However, it is important to stress that the coefficients α, β and also the noise σ^2 are now input dependent, being functions of the input parameters λ and ω.

10

III. INPUT-OUTPUT PROPERTIES OF THE JACOBI NEURONAL MODEL

A. Firing rate

The relation between the level of synaptic input received by a neuron and the frequency of the generated action potentials (firing frequency) is commonly reflected by the so-called f-I curve. The activation of an inhibitory input can produce in the neuron a change in its membrane potential (hyperpolarization) and/or an increase in the membrane conductance (shunting inhibition)[38,39]. The latter effect modifies the sensitivity of a neuron to a variation in the excitatory input rate[40] and produces a change in the slope of the f-I curve for different inhibitory input rates (*divisive effect*)[36]. If the slope is high, a small variation in the excitatory input rate produces a big difference in the resulting firing rate. The hyperpolarization decreases the membrane depolarization reducing the effect of a subsequent excitatory stimulation. In this case the f-I curve shifts for different inhibitory input rates but keeps its slope (*subtractive effect*). In this section, we investigate how the dependence of the coefficients α, β, σ in the model (14) on the input rates given by Eqs. (16) and (20) affects the FPTs (and thus the ISIs) of the Jacobi neuronal model.

As already mentioned, the firing frequency is commonly replaced by the inverse of the mean ISI, $1/\mathbb{E}(T)$. In this way we constructed the f-I curve for model (14) considering the same physiologically realistic parameters as those given in Example 1 of Ref. 21: $V_I = -10\text{mV}, V_E = 100\text{mV}, S = 10\text{mV}, \tau = 5.8\text{ms}, i = -0.2, a = 0.02, x_0 = 0\text{mV}$, for different values of ϵ, λ and ω, namely $\lambda \in (0, 3), \omega \in (0, 1)$ and $\epsilon = 0.001, 0.0145$ (as in Ref. 36), and 0.02.

In Fig. 2 we plot the firing rate as a function of the excitatory rate λ for different values of the inhibitory rate ω, and observe a divisive effect of inhibition for low frequencies of the excitatory input and a subtracting effect for high frequencies. For higher values of λ, the deterministic force characterized by β drives the neuron to fire. The behavior of $1/\mathbb{E}(T)$ for the neuronal model (14) differs from that of the general Jacobi diffusion (6) reported in Fig.1. There the inverse mean FPT increases when σ^2 increases, while here the firing rate decreases in the suprathreshold regime if we increase σ^2 by increasing the inhibitory rate, ω (cf. Eq.(16)).
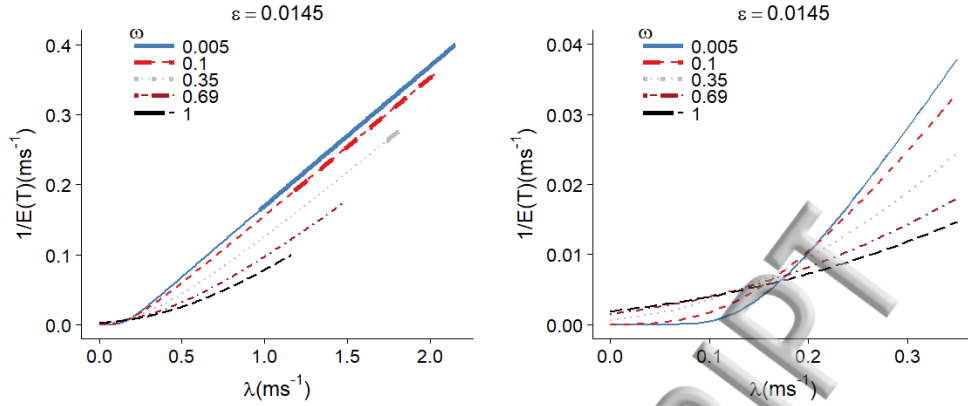
11

FIG. 2. Firing rate, $1/\mathbb{E}(T)$, for the Jacobi diffusion neuronal model, as a function of the excitatory rate λ for several fixed levels of the inhibitory rate ω, the values of λ are limited by condition (19). The right panel is a zoomed version of the left one. Same parameter values of Example 1 of Ref.21: $V_I = -10$ mV, $V_E = 100$ mV, $S = 10$ mV, $\tau = 5.8$ ms, $i = -0.2$, $a = 0.02$, $x_0 = 0$ mV, and $\epsilon = 0.0145$ as in Ref. 36. The values of ω are in the legend (ms^{-1}). We note a divisive effect for low frequencies and subtracting effect for high frequencies of the excitatory input, as also shown in Ref.36. The lines become thick when the chosen parameters yield the process in suprathreshold regime.

If we decrease the value of the reversal potential V_E, the excitatory term $\mu(V_E - X_t)$ in (14) has a weakened effect (figure not shown). The f-I curve shifts to the right for increasing inhibition ω compared to the case of Fig.2. This is because changing the reversal potential is equivalent to change the input by a constant quantity[41]. Also in this case, divisive and subtractive effects are observed. Thus, their presence does not depend on the value of the reversal potential.

B.   Firing variability

Using Eqs. (11) and (12), in Fig.3, we plot the CV of the ISIs generated by model (14) as a function of the excitatory rate λ for different fixed values of the inhibitory rate ω. In all the considered cases, the CV grows with increasing inhibition. For $\epsilon = 0.001$, it means very small level of noise, as seen from equation (16), the CVs are smaller than one and are decreasing functions of the excitatory rate λ. For bigger ϵ, we observe values of the
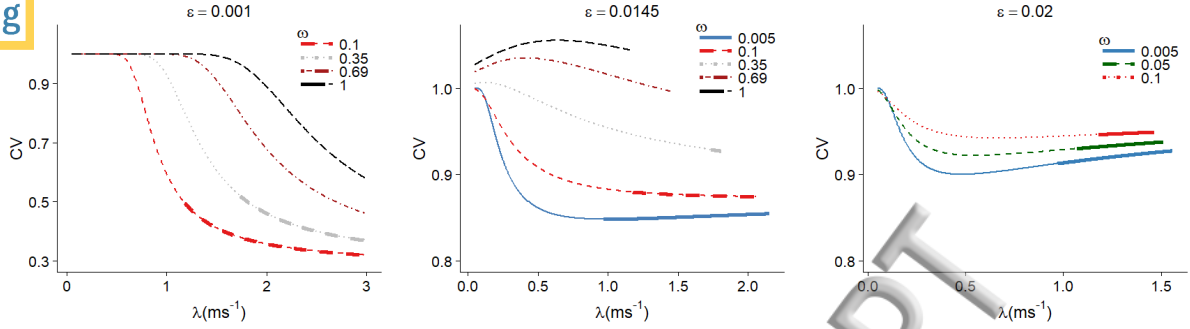
12

FIG. 3. Coefficient of variation of the ISIs generated by the Jacobi diffusion neuronal model as a function of the excitatory rate λ for several choices of the inhibitory rate ω. The parameters are chosen as in Fig.2. Left figure: $\epsilon = 0.001$. The CVs monotonically decrease in λ and takes small values for low inhibitory inputs. Central figure: $\epsilon = 0.0145$. The CVs grow with increasing inhibition. For high values of ω, the curves reach a maximum value and then change concavity. Right figure: $\epsilon = 0.02$. For values of ω close to zero, the CV curves have minima. All CVs are plotted as a function of λ such that Eq.(19) is fulfilled, this is the reason why some lines stop before others. The lines become thick when the chosen parameters yield a process in suprathreshold regime. All maxima and minima occur in the subthreshold regime in the considered cases.

CV greater than one and different behaviors, concavities and types of monotonicity of the CV for different values of ω. Interestingly, the CVs are non-monotonic in λ and some CVs exhibit a maximum or a minimum for certain values of the input parameters. Note that, in the cases considered here, all maxima and minima occur in the subthreshold regime (the thick lines in the figure indicate suprathreshold regime). Many of these features are not present in the CVs of the Jacobi diffusion (6) reported in Fig. 1, suggesting a qualitative difference between the general and the neuronal-based models.

To illustrate the simultaneous dependence of the CV on the inhibitory and the excitatory inputs, we report its heat map in Fig.4-left for $\epsilon = 0.0145$. All CVs increase in ω, CVs larger than one can be obtained by either increasing the inhibitory inputs or decreasing the excitatory inputs, while CVs smaller than one are only observed for low values of ω. Interestingly, for a fixed inhibitory input ω, it is possible to decrease the CVs by either increasing the excitatory input (as one would expect), or decreasing it. The blue lines report the contour plots of the CVs, i.e. the values of (λ, ω) yielding the same CVs, while the black dots represent the values of λ, denoted by λ^*, maximizing the CV for a fixed ω.
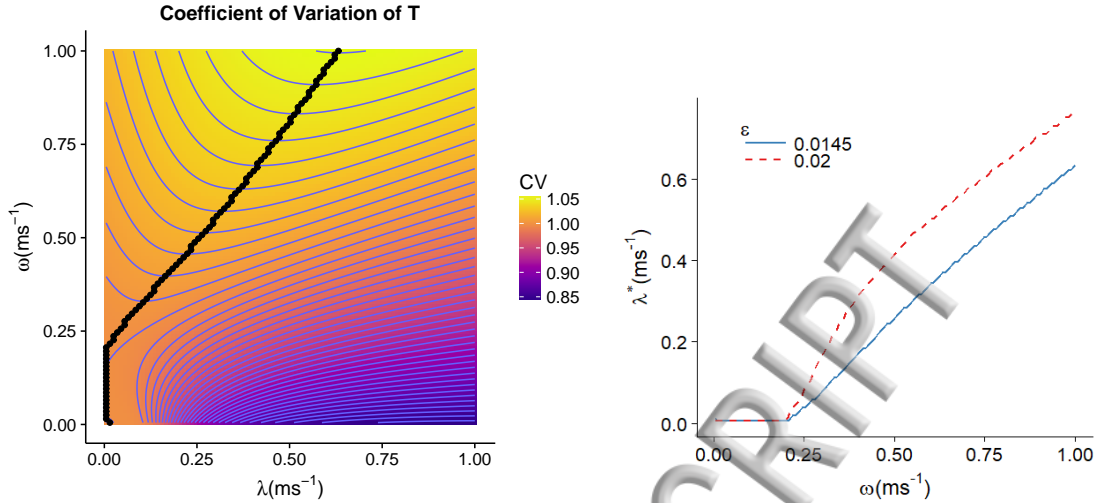
13

FIG. 4. Left figure: Heat map of the dependency of the CV of T on both inhibitory and excitatory inputs. The ranges of values of λ and ω are written on the axes labels, the other parameters are the same of Fig.2. The yellowish areas represent values of the CV larger than one. The blue lines are the curves along which the CV has a constant value, i.e. the 2D sections of the 3D plot (contour lines). The black points are (λ^*, ω), where λ^* denotes the value of λ maximizing the CV of T for a given ω. Right figure: Relationship between ω and λ^* for two different values of ϵ. Note that λ^* increases for increasing absolute values of ω; however the relation is not always linear as it may look from the heat map.

The values of λ^* increase with ω, suggesting some relation in the proportion of inhibitory and excitatory inputs. This can be observed in Fig.4-right, where we report (ω, λ^*) for two values of ϵ.

C. The role of input-dependent parameters

What is the reason causing the different behavior of the inverse mean FPT (firing rate) and the $\mathrm{CV}(T)$ for the Jacobi diffusion (6) and the neuronal model (14)? To answer this question, we investigate the role played by the inhibitory and excitatory inputs ω and λ in the coefficients α, β and σ^2 of the neuronal model (14). In the general Jacobi model (6), if seen as a neuronal model, the only variable coefficient is β, while in (14) the inputs affect all three coefficients. To answer the question posed above, keeping the notation of Section II B, we study how $1/\mathbb{E}(T)$ and $\mathrm{CV}(T)$ change if the input parameters act only on two of the

14

three coefficients.

In the first row of Fig.5, we fix $\alpha = 1/\tau$ constant, i.e., independent on the input parameters. Under this scenario we observe, except for very low values of ω, a small subtractive effect in the f-I curve for low values of λ. Almost no effect is seen for high values of λ. It suggests that the noise alone cannot produce large divisive effects. Similarly, no divisive effects are observed when $\alpha = 1/\tau + \mu$, i.e. when α depends on the excitation only ($\mu = a\lambda$) but not on the inhibition (results not shown). In contrast to Fig.2, the firing rate increases with the inhibition in this case. This is because the parameter ω effects σ^2 only, and in this way increases the fluctuations of the membrane depolarization and thus the firing rate. On the right panel of the first row of Fig.5, one can see that the CV increases when the rate of inhibitory input, ω, increases and is monotonically decreasing function of λ. These results agree qualitatively with what we observed in Fig.1 for the Jacobi diffusion (6).

In the second row of Fig.5, we let α and β vary with the input parameters and fix $\sigma^2 = 0.33$ ms^{-1}, physiological value used in Ref.21. A divisive effect is not visible in the f-I curve, while the subtractive one is strong. In this scenario, the firing rate decreases if the inhibitory rate increases. The CVs are monotonically decreasing functions of λ that intersect for different values of ω. For λ and ω close to zero, the CV is greater than one because, differently from before, σ^2 does not depend on them and therefore it does not tend to zero. Interestingly, increasing the inhibition reduces the CVs for values of λ smaller than 0.5 ms^{-1}.

In the third row of Fig.5, we consider $\beta = -V_I/(\tau(V_E - V_I))$ independent of λ, while α and σ^2 are varying with the input parameters. Both the divisive and the subtractive effects are visible in the f-I curve. However, the firing frequency, $1/\mathbb{E}(T)$, is lower than before (about $1/10$). Considering the dependency of CV on the input, we see that for values of ω greater than 0.1 ms^{-1}, the CV is monotonically increasing in λ and larger than one. This happens because β is constant while σ^2 increases in λ causing the variability to increase. Finally, under this scenario, for small values of ω (see the case $\omega = 0.01$ ms^{-1}) the CV curve shows a minimum, Fig.3 - right panel. To get maxima in the CV as a function of λ, it seems that the input parameters have to act simultaneously on all the three coefficients as happens for the Jacobi neuronal model (14) with coefficients given by Eq.(20).
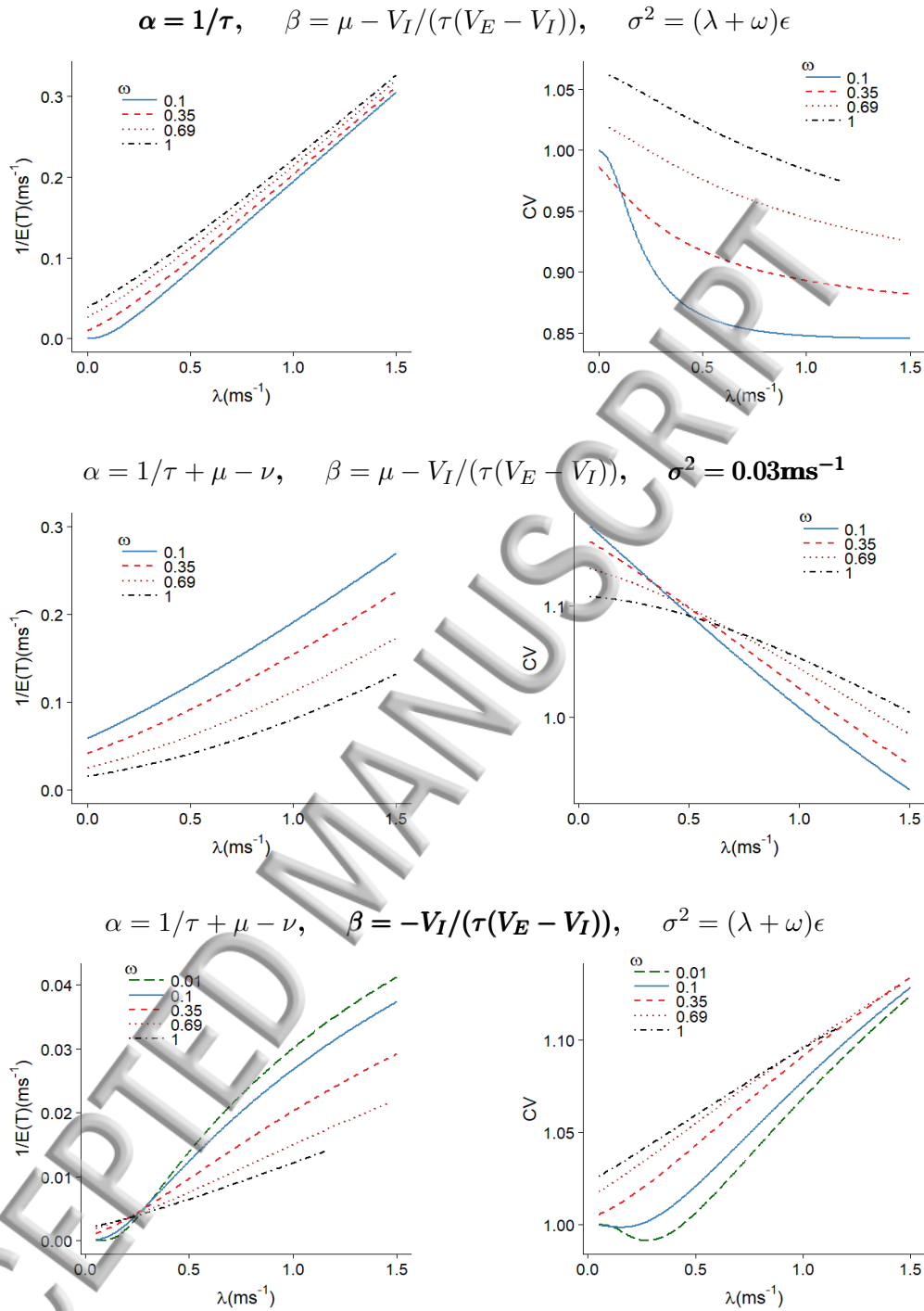
15

FIG. 5. Firing rate, $1/\mathbb{E}(T)$, and coefficient of variation of the ISIs generated by the Jacobi diffusion neuronal model as a function of the excitatory rate λ for several choices of the inhibitory rate ω if the input parameters act on two of the three coefficients α, β and σ^2 only (the constant one is marked in bold). In the first row $\alpha = 1/\tau$ constant (i.e. independent of the input parameters λ and ω), in the second row $\sigma^2 = 0.03$ ms^{-1} constant, in the third row $\beta = -V_I/(\tau(V_E - V_I))$ while α and σ^2 change with λ and ω. We recall from Eq. (15) that $\mu = a\lambda$ and $\nu = i\omega$.

IV. DISCUSSION

A. Firing rate

An increase of the firing frequency with increasing level of inhibition is a counter-intuitive phenomenon. It was observed for neuronal networks, e.g. in Ref.42, and for single neurons, e.g. in Ref.43. Here, for low values of the excitatory rate λ we see on the right panel of Fig.2 that increasing the inhibition increases the firing rate. The reason is the following: if the input frequency is low (small λ), then the inhibition helps the firing since it increases the noise, cf. Eq.(16).

The noise alone causes only a modest divisive effect on the firing rate during shunting inhibition. Holt and Koch[41] showed that for an integrate-and-fire model in the suprathreshold regime, the effect of a voltage-independent inhibition is subtractive. Doiron et al.[44] extended this result to the voltage-dependent case, observing a divisive effect at low frequencies of excitation for a stochastic leaky integrate-and-fire model with additive noise, provided that the noise increases with the inhibitory input[36]. Divisive modulation of the firing rate under noisy conditions is instead enhanced by a nonlinear integration of the inputs[45]. In fact, it is known that dendritic integration of excitatory and inhibitory inputs can be highly nonlinear due to the dendritic saturation[46]. In Ref.47 the authors proposed a dendritic integrate-and-fire model incorporating the nonlinearity of the dendritic integration rule, at the expense of an heavier mathematical formulation. The synaptic inputs are summed linearly in the original Stein's model[5], but the inclusion of the reversal potentials introduces a nonlinear synaptic summation. Here we argue that in neuronal models with multiplicative noise, like the Jacobi diffusion considered in Eq.(6) with parameters given by Eq.(20), a fundamental role to obtain divisive phenomena is played by the coefficient α, and in particular its dependence on the underlying inhibitory inputs. We speculate that, not only the role of the noise is crucial[48], but also $1/\alpha$ has to decrease for increasing ω to obtain a divisive effect (see third row of Fig.5).

B. Variability of the response

Traditionally, the neural code is assumed to be hidden in the firing frequency. Nevertheless, recently, the spiking variability attracts attention of neuroscientists as an alternative or

at least as an auxiliary part of the code[49–51]. Two interchangeable measures of variability, the Fano factor and the Coefficient of variation, have been employed[52–54]. Here, due to the knowledge of the first two moments of the ISIs, we evaluated the CV as a function of the excitation rate. It is drastically affected by the dependence of the coefficients α, β and σ^2 on the input parameters in Eq.(20) producing three main features: CV greater than one, and presence of maxima and minima with respect to the rate of excitatory inputs, λ.

We observe minima of CV for small values of the inhibitory rate and for strong dependency of the noise on the input (large values of ϵ). If the rate of inhibitory inputs, ω, is small, then an increase of λ implies a decrease in the CV, as it happens for the general Jacobi process with fixed α and σ^2. However, if the rate of excitatory inputs, λ, is large, the noisy term $\sigma^2 = (\lambda + \omega)\epsilon \approx \lambda\epsilon$ becomes dominant and the CV increases. Minima in the CV as a function of the noise were observed for the Ornstein-Uhlenbeck neuronal model[55].

In the Jacobi neuronal model with coefficients given by Eq.(20), the increase of inhibitory and excitatory rates leads to an increase of the noise σ^2, but at the same time to a decrease in $1/\alpha$ that reduces the voltage fluctuations. This suppression of fluctuations was also observed in the conductance-based model[14] and in vivo recordings[56]. This mechanism explains the presence of maxima in Fig.3: the CV grows with the noise but then it is slowed down by α. The maxima are not observed for $\epsilon = 0.001$, because in that case the noise is too small to produce an increase in the CV. To the best of our knowledge, maxima in the CV for the Ornstein-Uhlenbeck neuronal model were observed only when a refractory period was added to the dynamics[55].

Values of the CV larger than one are commonly found in experimental data and investigation of neuronal models in this direction has a long history[7,8]. Generally, it is perceived as connected to an increase of inhibition. Also for the Jacobi neuronal model with coefficients (20), the inhibition increases the CV. In fact, even if the inhibition causes an increase of the firing rate (and thus decreases the mean of T), it increases the variance of T even more substantially, producing thus a higher CV. Some authors connect large values of the CV with a balance between excitation and inhibition. For example, a highly irregular firing activity is produced in the presence of an appropriate balance of the excitatory and inhibitory input (see e.g. Ref.49 and Ref.57). Christodoulou and Bugmann[58,59] obtained CVs greater than one for strong inhibition, in particular for a level of inhibition that is greater than 80% of the level of excitation. Konig et al.[60] argued that an exact balance (100%) of excitatory and

inhibitory inputs cannot be realistic from a biological point of view. For the Jacobi neuronal model, we observe CVs greater than one also for the inhibitory rate that is less than 50% of the rate of the excitatory one, see for example Fig.3-central panel.

For all these reasons, the Jacobi neuronal model given by Eqs. (14), (16) and (20) constitutes a good compromise between the realistic description of a neuron and the mathematical tractability. Indeed, it is able to reproduce high degree of irregularity of the real neuronal firing. A deeper understanding of the meaning and consequences of minima and maxima in the CV of the ISIs is also of interest and it will be the object of a future work in the context of information transmission and coherence resonance.

ACKNOWLEDGMENTS

REFERENCES

[1] N. Brunel and M. C. W. van Rossum, Biological Cybernetics **97**, 337 (2007).

[2] N. Brunel and M. C. W. van Rossum, Biological Cybernetics **97**, 341 (2007).

[3] R. Jolivet, T. Lewis, and W. Gerstner, J. Neurophysiol. **92**, 959 (2004).

[4] W. Kistler, W. Gerstner, and J. vanHemmen, Neural Comput. **9**, 1015 (1997).

[5] R. Stein, Biophysical Journal **7**, 37 (1967).

[6] P. I. M. Johannesma, "Diffusion models for the stochastic activity of neurons," in *Neural Networks: Proceedings of the -School on Neural Networks - June 1967 in Ravello*, edited by E. R. Caianiello (Springer Berlin Heidelberg, Berlin, Heidelberg, 1968) pp. 116–144.

[7] H. C. Tuckwell, Journal of Theoretical Biology **77**, 65 (1979).

[8] W. J. Wilbur and J. Rinzel, Journal of Theoretical Biology **105**, 345 (1983).

[9] F. B. Hanson and H. C. Tuckwell, J. Theor. Neurobiol. **2**, 127 (1983).

[10] C. E. Smith and M. V. Smith, J. Theor. Neurobiol. **3**, 167 (1984).

[11] P. Lansky and V. Lanska, Biological Cybernetics **56**, 19 (1987).

19

[12]G. D'Onofrio, P. Lansky, and E. Pirozzi, Chaos: An Interdisciplinary Journal of Nonlinear Science **28**, 043103 (2018).

[13]M. Musila and P. Lansky, Journal of Theoretical Biology **171**, 225 (1994).

[14]M. J. E. Richardson, Phys. Rev. E **69**, 051918 (2004).

[15]M. J. E. Richardson and W. Gerstner, Chaos: An Interdisciplinary Journal of Nonlinear Science **16**, 026106 (2006).

[16]J. Cupera, Mathematical Biosciences and Engineering **11**, 11 (2014).

[17]B. Øksendal, *Stochastic Differential Equations: An Introduction with Applications*, Hochschultext / Universitext (Springer, 1998).

[18]J. Forman and M. Sørensen., Scandinavian Journal of Statistics **35**, 438 (2008).

[19]S. Karlin and H. Taylor, *A Second Course in Stochastic Processes*, v. 2 (Academic Press, 1981).

[20]A. J. F. Siegert, Phys. Rev. **81**, 617 (1951).

[21]V. Lanska, P. Lansky, and C. E. Smith, Journal of Theoretical Biology **166**, 393 (1994).

[22]N. Goel and N. Richter-Dyn, *Stochastic Models in Biology* (Academic Press, 1974).

[23]R. K. S. Hankin, *hypergeo: The Gauss Hypergeometric Function* (2016), R package version 1.2-13.

[24]R Core Team, *R: A Language and Environment for Statistical Computing*, R Foundation for Statistical Computing, Vienna, Austria (2013).

[25]D. Veestraeten, J. Appl. Probab. **52**, 595 (2015).

[26]J. Inoue, S. Sato, and L. M. Ricciardi, Biological Cybernetics **73**, 209 (1995).

[27]S.Shinomoto, Y.Sakai, and S.Funahashi, Neural Comput. **11**, 935 (1999).

[28]S. Ditlevsen and P. Lansky, Phys. Rev. E **76**, 041906 (2007).

[29]Q. Qin, J. Wang, H. Yu, B. Deng, and W. Chan, Chaos: An Interdisciplinary Journal of Nonlinear Science **26**, 063121 (2016).

[30]V. Lanska and P. Lansky, Biosystems **48**, 123 (1998).

[31]H. Tuckwell, *Introduction to Theoretical Neurobiology: Volume 2, Nonlinear and Stochastic Theories* (Cambridge University Press, 2005).

[32]L. Wolff and B. Lindner, Phys. Rev. E **77**, 041913 (2008).

[33]M. Tamborrino, L. Sacerdote, and M. Jacobsen, Physica D: Nonlinear Phenomena **288**, 45 (2014).

[34]G. A. Cecchi, M. Sigman, J.-M. Alonso, L. Martínez, D. R. Chialvo, and M. O. Magnasco,

20

Proceedings of the National Academy of Sciences **97**, 5557 (2000).

[35]P. Lansky and L. Sacerdote, Physics Letters A **285**, 132 (2001).

[36]A. Longtin, B. Doiron, and A. R. Bulsara, Biosystems **67**, 147 (2002).

[37]S. Koyama and R. Kobayashi, Mathematical Biosciences and Engineering **13**, 537 (2016).

[38]A. Destexhe, M. Rudolph, and D. Paré, Nature Reviews Neuroscience **4**, 739 (2003).

[39]W. Paulus and J. C. Rothwell, The Journal of Physiology **594**, 2719.

[40]S. J. Mitchell and R. Silver, Neuron **38**, 433 (2003).

[41]G. R. Holt and C. Koch, Neural Computation **9**, 1001 (1997).

[42]M. V. Tsodyks, W. E. Skaggs, T. J. Sejnowski, and B. L. McNaughton, Journal of Neuroscience **17**, 4382 (1997).

[43]J. Feng and G. Wei, Journal of Physics A: Mathematical and General **34**, 7493 (2001).

[44]B. Doiron, A. Longtin, N. Berman, and L. Maler, Neural Computation **13**, 227 (2001).

[45]S. A. Prescott and Y. De Koninck, Proceedings of the National Academy of Sciences **100**, 2076 (2003).

[46]D. Zhang, Y. Li, M. Rasch, and S. Wu, Frontiers in Computational Neuroscience **7**, 56 (2013).

[47]D. Zhou, S. Li, X.-h. Zhang, and D. Cai, PLOS ONE **8**, 1 (2013).

[48]F. S. Chance, L. Abbott, and A. D. Reyes, Neuron **35**, 773 (2002).

[49]M. N. Shadlen and W. T. Newsome, Current Opinion in Neurobiology **4**, 569 (1994).

[50]L. Kostal, P. Lansky, and J.-P. Rospars, European Journal of Neuroscience **26**, 2693 (2007).

[51]A. K. Churchland, R. Kiani, R. Chaudhuri, X.-J. Wang, A. Pouget, and M. Shadlen, Neuron **69**, 818 (2011).

[52]J. W. Shuai, S. Zeng, and P. Jung, Fluctuation and Noise Letters **02**, L139 (2002).

[53]M. P. Nawrot, "Analysis and interpretation of interval and count variability in neural spike trains," in *Analysis of Parallel Spike Trains*, edited by S. Grün and S. Rotter (Springer US, Boston, MA, 2010) pp. 37–58.

[54]K. Rajdl, P. Lansky, and L. Kostal, Neural Networks **95**, 57 (2017).

[55]B. Lindner, L. Schimansky-Geier, and A. Longtin, Phys. Rev. E **66**, 031916 (2002).

[56]C. Monier, F. Chavane, P. Baudot, L. J. Graham, and Y. Fregnac, Neuron **37**, 663 (2003).

[57]J. Feng and D. Brown, Biological Cybernetics **80**, 291 (1999).

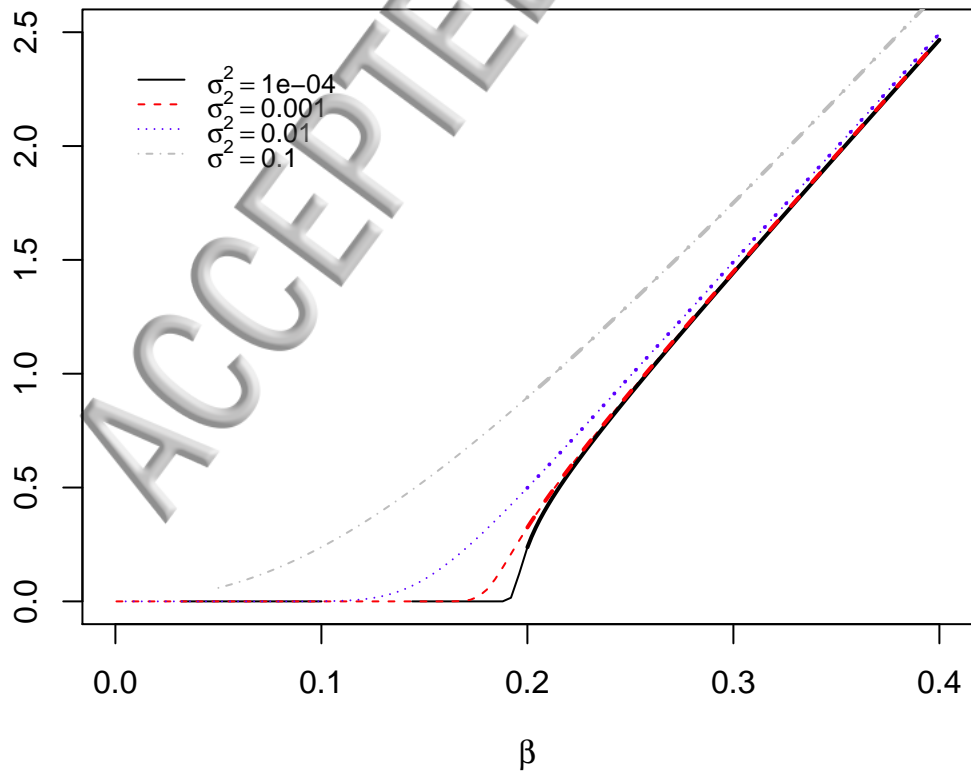[58]C. Christodoulou and G. Bugmann, Biosystems **58**, 41 (2000).

[59]C. Christodoulou and G. Bugmann, Neurocomputing **38-40**, 1141 (2001), computational Neuroscience: Trends in Research 2001.

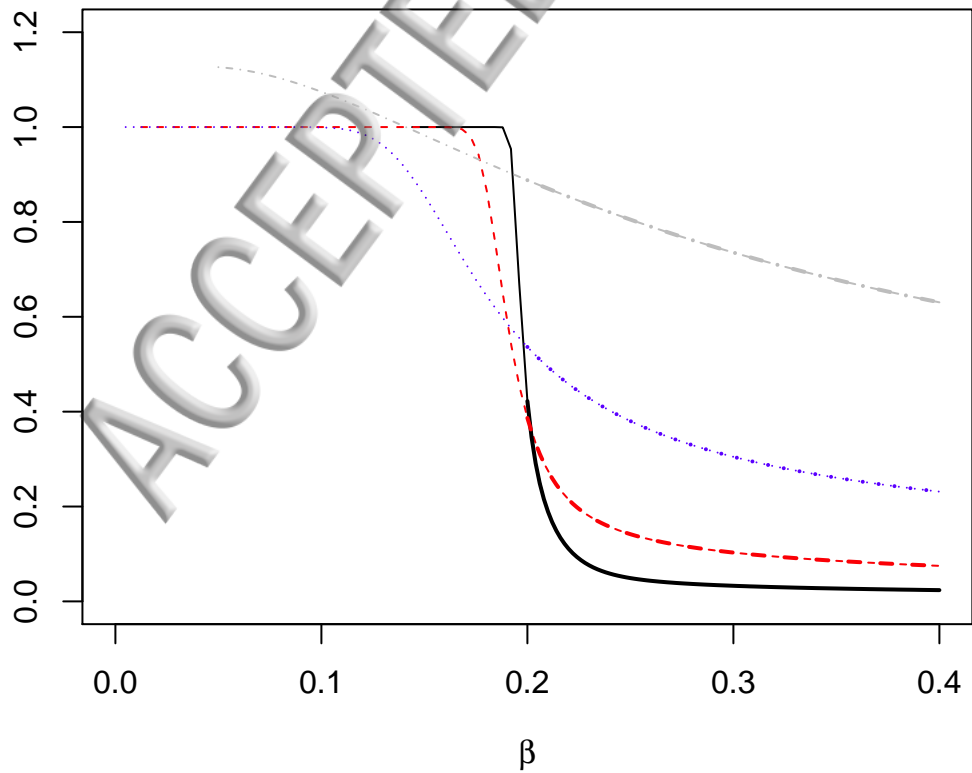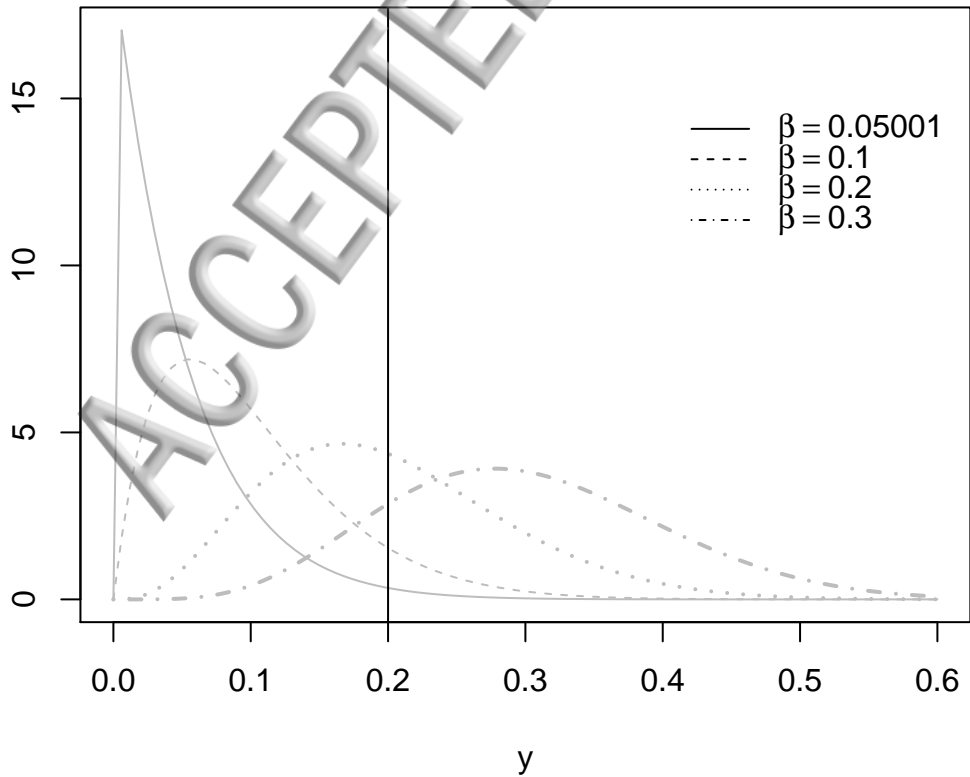[60]P. Konig, A. K. Engel, and W. Singer, Trends in Neurosciences **19**, 130 (1996).

a)

b)

c)

pdf of Y_∞

y

β = 0.05001
β = 0.1
β = 0.2
β = 0.3

$\varepsilon = 0.0145$

Legend: ω
- 0.005
- 0.1
- 0.35
- 0.69
- 1

$\varepsilon = 0.001$
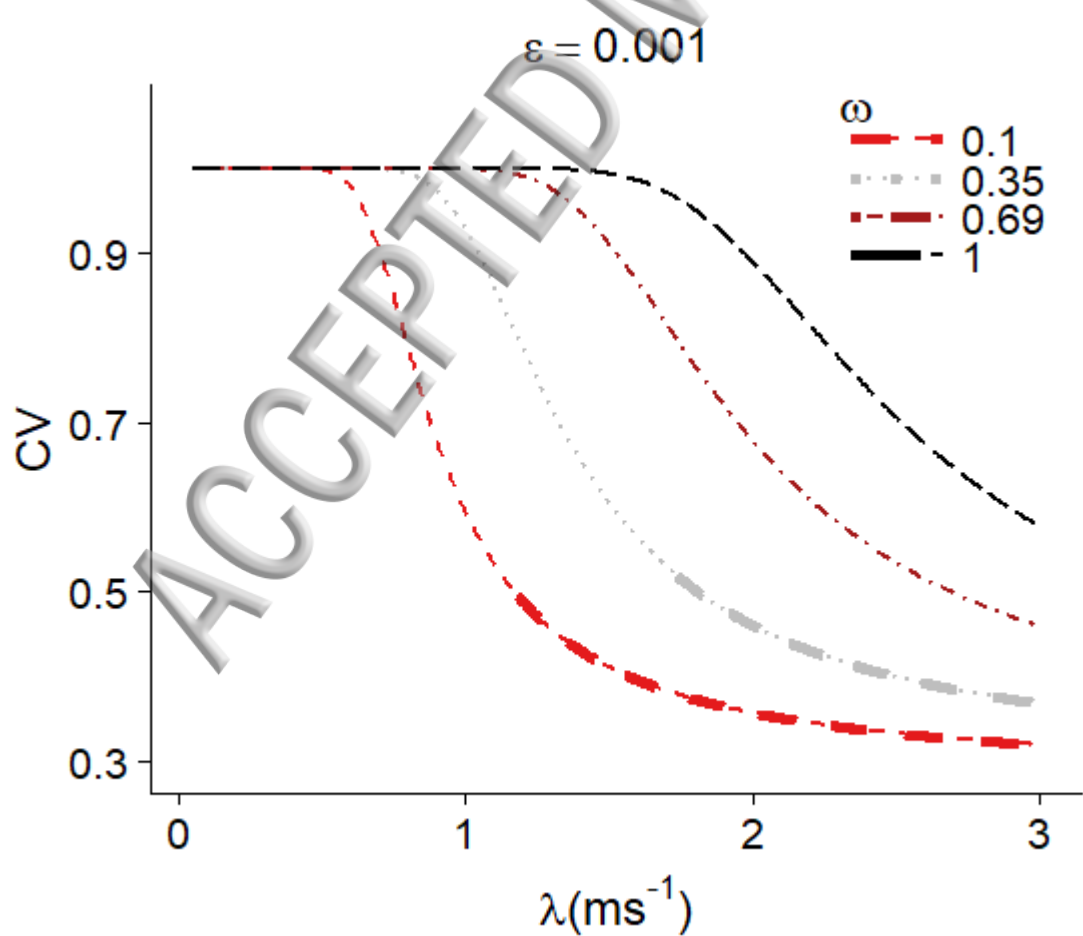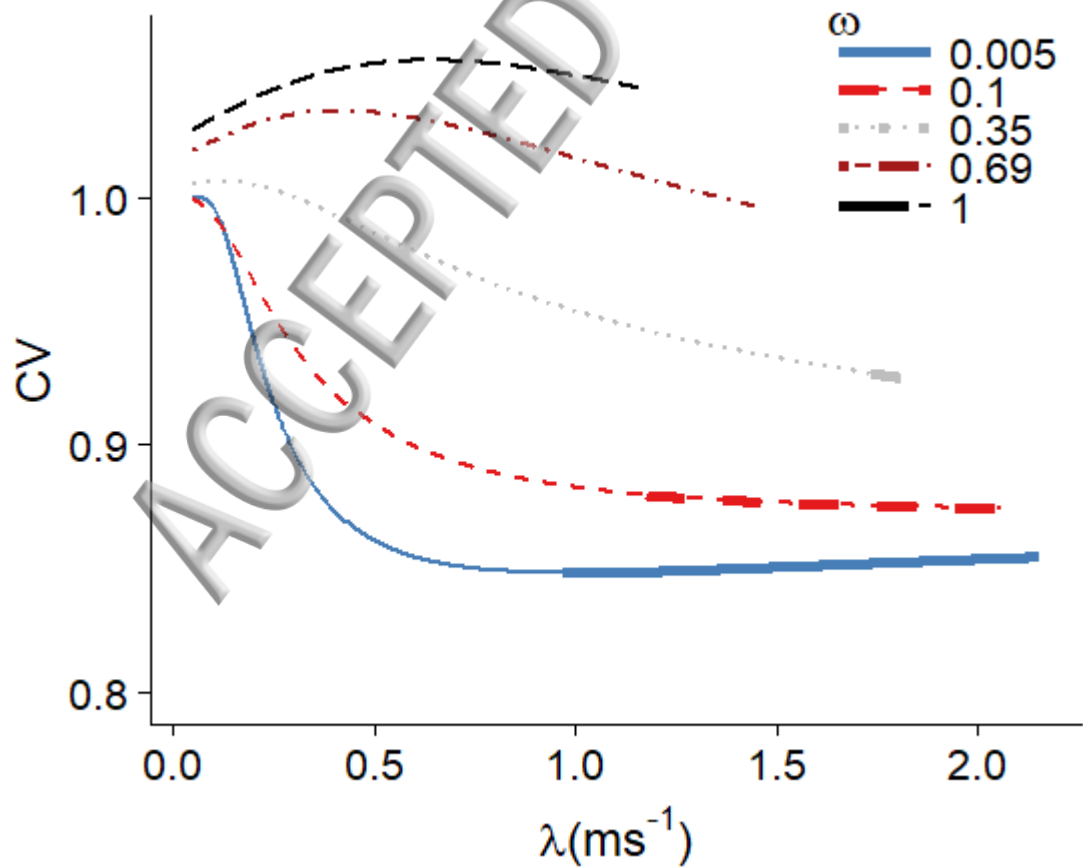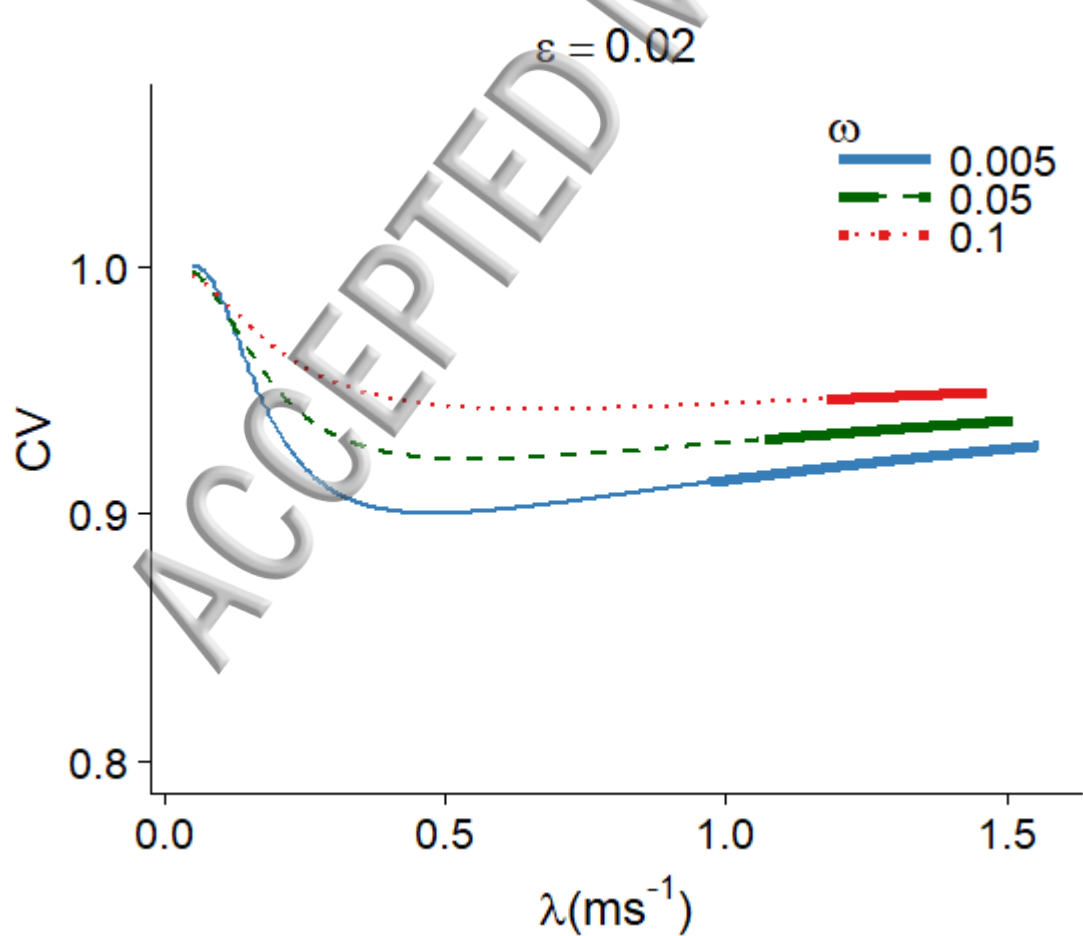
ω
- - - 0.1
········· 0.35
-·-·- 0.69
- - - 1

$\epsilon = 0.0145$

$\varepsilon = 0.02$

Coefficient of Variation of T

Legend:

ε
0.0145 (blue solid line)
0.02 (red dashed line)